

Accepted Article

Title: Chloride-induced highly active Au catalyst for methyl esterification of alcohols

Authors: Chengming Zhang *, Yongzhao Wang

This manuscript has been accepted and appears as an Accepted Article online.

This work may now be cited as: *Chin. J. Chem.* **2019**, *37*, 10.1002/cjoc.201800374.

The final Version of Record (VoR) of it with formal page numbers will soon be published online in Early View: <http://dx.doi.org/10.1002/cjoc.201800374>.

Chloride-induced highly active Au catalyst for methyl esterification of alcohols

Chengming Zhang *, Yongzhao Wang

Engineering Research Center of Ministry of Education for Fine Chemicals, School of Chemistry and Chemical Engineering, Shanxi University, Taiyuan 030006, China

Abstract

Chloride is generally regarded as a harmful species for the heterogeneous catalysts, especially Au catalysts. In this work, a series of active Au/NiOx catalysts were successfully prepared with co-precipitation method by tracking the concentrations of chloride in the re-dispersed aqueous solutions. For methyl esterification of alcohols, the highest active Au/NiOx catalysts could be prepared from aqueous solutions containing 8-13ppm chloride, the yield of methyl benzoate of catalyst Au/NiOx-9 was 99%. The catalyst structures and the role of chloride in catalysts were explored by ICP, BET, XPS, TEM and EXAFS characterizations. It was found that the appropriate amount of residual chloride in Au catalysts was beneficial to their catalytic activities. Especially for Au/NiOx-9, the appropriate amount of residual chloride had positive effects on the physicochemical properties of Au/NiOx catalyst, the position of Au nanoparticles (NPs) located on NiOx crystallites and the ratio of Au^{δ+}/Au⁰ in catalyst, which together resulted in its high reactivity.

Keywords: Au catalyst; preparation; chloride; esterification

Introduction

In recent decades, Au catalysts have received growing attentions and been widely applied in many important research fields [1] since good performance of Au catalysts was discovered [2-6]. However, the controllable preparation of highly active

This article has been accepted for publication and undergone full peer review but has not been through the copyediting, typesetting, pagination and proofreading process, which may lead to differences between this version and the Version of Record. Please cite this article as doi: 10.1002/cjoc.201800374

This article is protected by copyright. All rights reserved.

heterogeneous catalysts is still a longstanding challenge till now, especially Au catalysts. Many efforts have been devoted to this problem. The active site, structure and the quantum size effect of Au catalyst [7, 8], active oxygen species of the support [9, 10], suitable reducible oxide supports [11], and so on, have been extensively studied. Additionally, catalyst precursors, bases, pH value, aging time, and calcination temperature are also crucial conditions [2, 12-18]. Nevertheless, the controllable preparation of highly active Au catalyst is still difficult to realize even strictly following above conditions.

Chloride (usually as Cl^-) is generally regarded as a harmful species for Au catalyst, because of strong interaction of chloride and Au. However, in the light of the report that the active Au catalysts were prepared without chloride removing [19], it was deduced that the active Au catalyst may be possibly prepared in the presence of an appropriate amount of chloride. In our previous work, by finely tracing the chloride concentration in the re-dispersed aqueous solutions, we realized the reproducible preparation of Au/ Fe_2O_3 catalyst for CO oxidation [20]. It is meaningful to explore whether this method can be applied to other catalysts and reactions or not.

Methyl esterification reaction is one of the most fundamental transformations in organic synthesis reactions. And methyl esters are commercially valuable chemicals. Direct catalytic esterification of alcohols (or aldehydes) has been widely studied [21-23]. Yajuan Hao successfully synthesized uniform Au NPs by the nanocages of a mesoporous material. Au NPs were catalytically active in the oxidative esterification of straight-chain alcohols [24]. Huili Wei investigated Au/MgO was a highly efficient catalyst for methyl esterification reaction [23]. High concentration of basic sites on the support played a pivotal role in this catalytic esterification reaction [25, 26]. Guofeng Zhao found that large amounts of $\text{Ni}_2\text{O}_3\text{-Au}^+$ hybrid On NiOx@Au ensembles were highly active for the low-temperature oxidation of alcohols. Ni_2O_3 species not only promoted the formation of Au^+ ions and stabilized them but also served as an oxygen supplier to transfer oxygen species onto the Au^+ sites [27]. Ken Suzuki developed a novel supported Au-NiOx catalyst having a core-shell structure that could efficiently catalyze Aerobic oxidative esterification of methacrolein in

methanol to methyl methacrylate [28].

In this work, Methyl esterification of alcohols was chosen as model reaction. The active Au/NiOx catalysts were prepared by tracking the concentrations of chloride in the re-dispersed aqueous solutions. When the chloride concentrations were in the range of 8-13 ppm, active Au/NiOx catalysts for catalytic esterification of alcohols could be repeatedly obtained. The role of chloride in the formation of highly active Au catalysts has been preliminarily discussed in this article. Due to the non-detectability of residual chlorine in the final catalyst at low content, our discussions were based on the concentration of chlorine in the aqueous solution.

Results and Discussion

For esterification of benzyl alcohol, the catalytic activities of 15 Au/NiOx samples, which were prepared from the re-dispersed aqueous solutions with chloride concentrations in the range of 2 to 108 ppm, were studied. According to the results shown in Fig.1, the yields of methyl benzoate were less than 21% if the catalysts were prepared from aqueous solutions containing >22 ppm chloride. More active catalysts were obtained when the chloride concentrations continued to decrease. The highest active Au/NiOx catalysts could be prepared from aqueous solutions containing 8-13ppm chloride, the yield of methyl benzoate of catalyst Au/NiOx-9 was 99%. However, the catalysts turned less active again when the chloride concentrations were < 8 ppm. Typically, the yield of methyl benzoate was 20% with catalyst Au/NiOx-3. Combined with our previous work [20], the optimal chloride concentration range is different for the different reactions and different catalyst systems. However, if complying with the optimal the range of chloride concentration in aqueous solution, the highly active Au catalysts would be obtained reproducibly. For comparison, the catalytic activity of the sample Au/NiOx-0 prepared with gold hydroxide (Au(OH)₃) as the precursor was much less than Au/NiOx-9.

Table 1 Physicochemical properties of catalyst samples

Entry	Catalyst	Au Content(%) ^a	S _{BET} (m ² /g)	pore size (nm)	Surface [Cl] (wt%) ^b	Conversion of benzyl alcohol	Yield of methyl benzoate
1	Au/NiOx-3	2.90	238	6.3	0.40	20.5%	20%
2	Au/NiOx-9	2.96	226	7.4	0.52	99%	99%
3	Au/NiOx-22	3.07	221	9.6	0.89	22.3%	21%
4	Au/NiOx-0	3.1	231	9.3	--	68%	90%

^a Determined by ICP measurement; ^b Determined by XPS;

To check the relationships among the catalyst preparation operations, catalyst structure and catalytic activity, three typical samples, Au/NiOx-3, Au/NiOx-9 and Au/NiOx-22, with the yields of methyl benzoate 20%, 99% and 21% respectively, were characterized by ICP, BET, XPS, TEM and EXAFS. According to ICP analysis data, the Au loadings in these three samples were 2.90, 2.96 and 3.07 wt%, as shown in Table 1, indicating that the catalytic activity variation was not caused by Au loading.

The data of BET analysis for Au/NiOx-3, Au/NiOx-9 and Au/NiOx-22 are summarized in Table 1 and Fig. 2. The N₂ adsorption-desorption isotherms showed that the catalyst samples were all mesoporous materials. The BET surface areas of catalysts Au/NiOx-3, Au/NiOx-9 and Au/NiOx-22 were 238, 226 and 221 m²/g, and the pore size were 6.3, 7.4 and 9.6 nm, respectively. As shown in Fig 2, whether adsorption process or desorption process, the N₂ adsorption quantity of the sample Au/NiOx-9 was higher than that of Au/NiOx-3 and Au/NiOx-22 under the same pressure. Although the sample Au/NiOx-9 had no the highest specific surface area, it had the highest catalytic activity. It could be concluded that the sample Au/NiOx-9 with the best catalytic performance should have more effectively adsorption sites in the catalyst surface. These results suggested that the changing chloride concentration in aqueous solution definitely influenced the physicochemical properties of Au/NiOx. Accordingly, the appropriate physicochemical properties of Au catalyst should be a most important factor that led to active Au/NiOx catalysts.

To obtain further information about the chemical states of Au/NiOx, XPS measurements were performed for three representative catalysts Au/NiOx-3,

Au/NiOx-9 and Au/NiOx-22. As shown in Fig. 3a, Au species existed in the Au/NiOx had two forms, metallic gold (Au^0) and positively charged gold ($\text{Au}^{\delta+}$). The peak at 84.1eV was attributed to Au^0 [30], and binding energy of $\text{Au}^{\delta+}$ was 84.8eV [26, 27, 29, 30]. The contents of $\text{Au}^{\delta+}$ in Au/NiOx-3, Au/NiOx-9 and Au/NiOx-22 were about 17, 29 and 42%, respectively. It can be concluded that the more chloride existed in the catalyst the more $\text{Au}^{\delta+}$ produced. Above results suggested that the chemical state of Au could be regulated by adjusting chloride concentration of the aqueous solution. The best performance was observed with Au/NiOx-9 catalyst. Maybe that was because the appropriate ratio of $\text{Au}^{\delta+}$ and Au^0 directly led to the strengthening polarization of electron clouds of Au NPs, and enhanced the ability to activate oxygen molecules.

According to the XPS data depicted in Fig. 3b, for all samples Au/NiOx, the typical binding energies of Ni^{2+} (854.4 eV) and Ni^{3+} (856.2eV) [27, 31, 32] were all observed. In spite of the change of chloride concentration in aqueous solution, the ratio of Ni^{2+} (854.3 eV) in the support remained constant ~30%. This result might stem from the controllable preparation process in which the other conditions maintained unchanged except for chloride concentration.

TEM measurement results of Au/NiOx are shown in Fig. 4. Their TEM images were similar and they all seemed amorphous. Three supports were aggregated by small NiOx crystallites in nanoscales. As depicted in Fig. 4, for the sample Au/NiOx-22, the lattice of Au could be observed and wrapped in NiOx crystallites. Au NPs in Au/NiOx-9 and Au/NiOx-3 were clearer in comparison to Au/NiOx-22. After minute investigation, for Au/NiOx-9, the most of Au NPs connected with the edges of NiOx crystallite or the junctions of several NiOx crystallites [33, 34]. In consideration of the best catalytic performance of this sample, this observation strongly supported the former results about active site in Au catalyst, i.e. the interface between Au and iron oxide [7]. This phenomenon was also observed in our previous work [20]. It suggested that the appropriate amount of chloride might act as the linkage between Au and the edge of NiOx crystallite to gain the active Au catalyst, For Au/NiOx-22 and Au/NiOx-3, too much or less chloride was presented, the

interaction of Au and NiOx like Au/NiOx-9 decreased significantly. Accordingly, the catalytic activity lost sharply. By metering more than 150 Au NPs, as given in Fig 4, the mean diameters of Au NPs in samples Au/NiOx-3, Au/NiOx-9 and Au/NiOx-22 were 4.1, 3.8 and 6.6 nm with 1.91, 1.84 and 3.06 standard deviations. The size distributions of Au NPs in Au/NiOx-3 and Au/NiOx-9 samples were extremely similar. The marked difference of catalytic activities of these two catalysts did not come from the size effect of Au NPs, but from the contact way of Au NPs and NiOx crystallites.

Fig. 5 shows Fourier transformed (FT) EXAFS spectra for three Au/NiOx and the standard samples. Similar EXAFS spectra were obtained from Au/NiOx-3, Au/NiOx-9 and Au/NiOx-22. Their EXAFS spectra peaks became broader in comparison with Au foil. Furthermore, according to EXAFS data analysis by ifeffit programs, Au-Cl bond was not found in all three samples. Further comparing three typical catalysts with standard samples of Au foil and gold trichloride, the peaks of three Au/NiOx samples between two dotted lines in Fig 6a shifted gradually to the position of Au-Cl bond with the increase of the chloride concentration. This result suggested that although no Au-Cl bond existed the presence of chloride did influence the chemical state of Au in catalyst and gave rise to the existence of a certain amount of positive gold. As shown in Fig 5b, NiOx supports of three samples Au/NiOx-3, Au/NiOx-9 and Au/NiOx-22 were the same, and this result reconfirms the observation from XPS characterization.

To date, there was still insufficient evidence to reveal the real role of chloride in the formation of the active Au catalyst. But, based on the known data, we could make some reasonable conjectures. First, as pH value of the mother aqueous solution rose, Au-Cl bond broke, and chlorine in chloroauric acid was substituted by the hydroxyl. And then, small Au NPs formed. Finally, chloride was adsorbed on the support NiOx or existed in aqueous solution. Because of strong interaction of chloride and Au, the presence of a major amount of chloride not only caused the agglomeration of Au NPs but also led to the coating effect of Au NPs by the support in the process of calcination. As shown in Fig. 6, when the content of chloride in Au catalysts continued to decrease with the ultrasonication and washing operations, chloride

adsorbed on the planes of NiOx crystallites was preferentially eliminated. Nevertheless, chloride located on the edges of NiOx crystallites still remained. It was the residual chloride that induces Au NPs to anchor on the edges of NiOx crystallites. If excessive ultrasonication and washing operations were carried out, chloride located on the edges of NiOx crystallites disappeared entirely, and the guiding effect of chloride did not exist. So, most of Au NPs were inclined to anchor on the planes of NiOx crystallites or located between different planes, and the activity of the catalyst dropped sharply.

The catalytic mechanism of methyl esterification of alcohols is as follows: First, the alcohol molecules were adsorbed on the support surface to weaken the O-H bonds of the alcohols [35]. The α -H was attracted by the O₂ activated on the Au NPs surface. Then, the α -H was removed, forming an oxygen-carbon double bond. And then, another alcohol (CH₃OH) rapidly undertook a nucleophilic addition reaction to form hemiacetal. Finally, the α -H of alcohol and the hydrogen in hydroxyl group of hemiacetal formed H₂O with the activated O₂. Concurrently, the final product was obtained [36-38]. As we all known, the alcohol molecules were preferentially adsorbed on the edges of NiOx crystallites where there are abundant defective sites. If Au NPs located at the same position, the adsorption sites of alcohols would act synergistically with the activation sites of oxygen molecules because of the short distance. This synergetic effect caused by chloride might be another important factor that influenced catalytic activity.

Au/NiOx-9 was chosen to test the generality of the Au/NiOx catalysts for the methyl esterification reaction, and the results are shown in table 2. For benzyl alcohol, the catalytic activity of Au/NiOx-9 was excellent (entry1), and the conversion and the selectivity both reached 99%. For F and Cl substituent (entry4, 5), the conversion of fluorobenzyl alcohol and chlorobenzyl alcohol was 95% and 90%, and their selectivity was 93%, 91%, respectively. The substrates with electron-withdrawing groups, such as F, Cl, NO₂, CF₃ (entry 4, 5, 6, 8) and electron-donating group (entry 2, 3, 7), all tended to obtain high catalytic activity. Additionally, furfural afforded the desired ester product in 93% conversion and 96% selectivity.

Table 2. Esterification of methanol and other alcohols over Au/NiOx-9

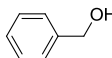
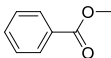
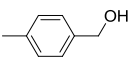
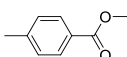
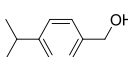
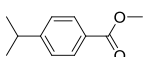
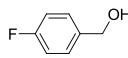
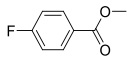
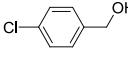
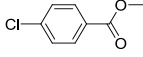
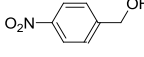
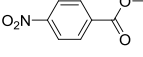
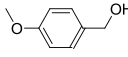
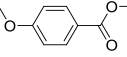
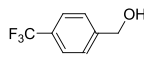
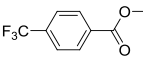
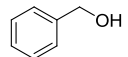
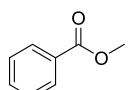
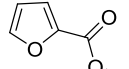
entry	substrates	products	Conversion%	Selectivity%
1			99	99
2			99	98
3			99	96
4			95	93
5			90	91
6			99	90
7			95	85
8			90	98
9			93	96

Table 3 Comparison between Au/NiOx-9 and the related catalysts in literatures

catalyst	substrate	product	additive	Yield %	reference
Ag-MPTA-1			K ₂ CO ₃	95	[35]
Au/CeO ₂			Cs ₂ CO ₃	99	[36]
Au/CeO ₂			--	12.6	[36]
Au/TiO ₂			Cs ₂ CO ₃	76.3	[36]
Au/MgO				86	[25]
Pd/Cu ₂ Cl(OH) ₃			TBHP ^a	71	[37]
Au-Pd/MSN			K ₂ CO ₃	99	[38]
Au/NiOx			--	99	This work
Au/CMK-3			TBHP ^a	75.2	[39]
Co-N-C/MgO			K ₂ CO ₃	94.8	[40]
Au/NiOx			--	88.4	This work

^a used as oxidant

Table 1 compares Au/NiOx-9 catalyst with some reported catalysts. It could be seen that Au/NiOx had an excellent catalytic activity compared with other reported

catalysts. In brief, controlling the chloride concentrations in the re-dispersed aqueous solution was an effective method to obtain the active Au catalyst.

Conclusions

In summary, by tracing the chloride concentrations in the re-dispersed aqueous solution, we successfully prepared active Au/NiOx catalyst for catalytic methyl esterification of alcohols. If the chloride concentration was not in the range of 8-13ppm, the catalytic activity dropped dramatically. These results indicated that the presence of appropriate amounts of residual chloride was beneficial to obtain highly active heterogeneous catalysts. According to the known data, it may be inferred that a very small amount of residual chloride in Au catalyst had the guiding effect which induced Au NPs to anchor on the edges of NiOx crystallites. Thus, the synergistic effect of alcohol adsorption site and oxygen activation site is produced. In addition, the ratio of $\text{Au}^{\delta+}/\text{Au}^0$ in catalysts and the textural properties of Au/NiOx catalyst were also the important factors which affected catalytic activities. This work can offer a new perspective to realize the controllable preparation of active heterogeneous catalysts.

Experimental details

20 mL $\text{Ni}(\text{NO}_3)_2 \cdot 6\text{H}_2\text{O}$ (0.011 M) and 1.05 mL HAuCl_4 (0.24 M) were mixed together and were dropwise added into 60 mL Na_2CO_3 solution (0.31 M) under vigorous stirring in 0.5 h. It was further stirred for 3 h. The turbid liquid was divided into four sections and separation by centrifugation. Each section of the recovered precipitate was re-dispersed in different amount of deionized water and ultrasonically washed for 1 h. The chloride concentration in the re-dispersed aqueous solution of each section was determined by potentialstatic scanning method with a CHI660D electrochemical workstation. Then, the solid was separated by centrifugation, dried at 80 °C for 3 h and calcined at 350 °C for 0.5 h to produce the catalyst sample, which was denoted as Au/NiOx-X, in which X suggested the chloride concentration in ppm.

For comparison, Au/NiOx-0 was prepared with Gold hydroxide ($\text{Au}(\text{OH})_3$) as the precursor.

1mmol benzyl alcohol, 30 mg catalyst and 2 mL methanol were added into a glass tube. And then it was exchanged with oxygen and reacted at 60 °C (1 atm, O_2 balloon). After reaction, it was cooled to room temperature. Biphenyl was used as internal standard and a certain amount of ethanol were added into the reaction mixture up to 10mL for quantitative analysis by GC-FID (Agilent 7890A)

Catalyst characterization

TEM analysis was carried out on a Tecnai-G2-F30 field emission transmission electron microscope. The catalyst samples were dispersed in ethanol and ultrasonicated at room temperature for 0.5 h. A part of solution was dropped on the grid for the measurement of TEM images. XRD measurements are conducted by an X'Pert PRO (PANalytical) diffractometer. The XRD diffraction patterns were scanned in the 2θ range of 10-80°. The XPS measurements were performed with a Thermo scientific ESCALAB 250 instrument provided with a dual Mg/Al anode X-ray source, a hemispherical capacitor analyzer and a 5 keV Ar^+ ion-gun. All spectra were recorded using non-monochromatic Mg $\text{K}\alpha$ (1253.6 eV) radiation. Nitrogen adsorption-desorption isotherms were measured at 77 K using Micromeritics 2010 instrument. The pore-size distribution was calculated by Barrett, Joyner and Halenda (BJH) method from desorption isotherm. The Au loadings of the catalysts were measured by inductively coupled plasma-atomic emission spectrometry (ICP-AES), using an Iris advantage Thermo Jarrel Ash device. Extended X-ray absorption fine structure (EXAFS) experiments were performed at the Beijing Synchrotron Radiation Facility (BSRF) in Beijing Institute of High Energy Physics, Chinese Academy of Sciences with storage ring energy of 2.5 GeV and a beam current between 150 and 250 mA. EXAFS data analysis was carried out using ifeffit analysis programs (<http://cars9.uchicago.edu/ifeffit/>). Radial distribution functions were obtained by Fourier-transformed k_3 -weighted χ function.

Acknowledgement

This work was supported by the National Natural Science Foundation of China (grant number 21073208) and the CAS for financial support

***Corresponding author**

Tel.: +86 0351-7010588

E-mail address: zhangchm@sxu.edu.cn (C. Zhang)

Reference

- [1] R. Ciriminna, E. Falletta, Cristina Della Pina, J.H. Teles, M. Pagliaro, *Angew. Chem. Int. Ed.* **2016**, 55, 2.
- [2] M. Haruta, N. Yamada, T. Kobayashi, S. Iijima, *J. Catal.* **1989**, 115, 301.
- [3] A.S.K. Hashmi, G.J. Hutchings, *Angew. Chem. Int. Ed.* **2006**, 45, 7896.
- [4] B.K. Min, C.M. Friend, *Chem. Rev.* **2007**, 107, 2709.
- [5] A. Corma, H. Garcia, *Chem. Soc. Rev.* **2008**, 37, 2096.
- [6] J.L. Gong, C.B. Mullins, *Acc. Chem. Res.* **2009**, 42, 1063.
- [7] G.C. Bond, D.T. Thompson, *Gold Bull.* **2000**, 33, 41.
- [8] M. Valden, X. Lai, D.W. Goodman, *Science* **1998**, 281, 1647.
- [9] M. Kotobuki, R. Leppelt, D.A. Hansgen, D. Widmann, R.J. Behm, *J. Catal.* **2009**, 264, 67.
- [10] T. Fujitani, I. Nakamura, *Angew. Chem. Int. Ed.* **2011**, 50, 10144.
- [11] X. Xu, Q. Fu, X. Guo, X. Bao, *ACS Catal.* **2013**, 3, 1810.
- [12] S. Golunski, R. Rajaram, N. Hodge, G.J. Hutchings, C.J. Kiely, *Catal. Today* **2002**, 72, 107.
- [13] S.J. Lee, A. Gavriilidis, *J. Catal.* **2002**, 211, 283.
- [14] J. Guzman, B.C. Gates, *Angew. Chem. Int. Ed.* **2003**, 42, 690.
- [15] A. Hugon, N. El Kolli, C. Louis, *J. Catal.* **2010**, 274, 239.
- [16] L. Liu, B. Qiao, Z. Chen, J. Zhang, Y. Deng, *Chem. Commun.* **2009**, 6, 653.
- [17] L.Q. Liu, B.T. Qiao, Y.B. Ma, J. Zhang, Y.Q. Deng, *Dalton Trans.* **2008**, 19, 2542.
- [18] B.T. Qiao, Y.Q. Deng, *Chem. Commun.* **2003**, 17, 2192.
- [19] D.S. Pinnaduwage, L. Zhou, W. Gao, C.M. Friend, *J. Am. Chem. Soc.* **2007**, 129, 1872.
- [20] C. Zhang, L. Liu, X. Cui, L. Zheng, Y. Deng, *Sci. Rep.* **2013**, 3, 1503.

- [21] Chao Liu, Shan Tang, Liwei Zheng, Dong Liu, Heng Zhang, A. Lei, *Angew. Chem. Int. Ed.* **2012**, 51, 5662.
- [22] Chao Liu, Jing Wang, Lingkui Meng, Yi Deng, Yao Li, A. Lei, *Angew. Chem. Int. Ed.* **2011**, 50, 5144.
- [23] H. Wei, J. Li, J. Yu, J. Zheng, H. Su, X. Wang, *Inorg. Chim. Acta* **2015**, 427, 33.
- [24] Y. Hao, Y. Chong, S. Li, H. Yang, J. *Phys. Chem. C* **2012**, 116, 6512.
- [25] X. Wan, W. Deng, Q. Zhang, Y. Wang, *Catal. Today* **2014**, 233, 147.
- [26] M. Estrada, V.V. Costa, S. Beloshapkin, S. Fuentes, E. Stoyanov, E.V. Gusevskaya, A. Simakov, *Appl. Catal. A: General* **2014**, 473, 96.
- [27] G. Zhao, H. Hu, W. Chen, Z. Jiang, S. Zhang, J. Huang, Y. Lu, *Catal. Sci. Technol.* **2013**, 3, 404.
- [28] K. Suzuki, T. Yamaguchi, K. Matsushita, C. Iitsuka, J. Miura, T. Akaogi, H. Ishida, *ACS Catal.* **2013**, 3, 1845.
- [29] T. Wang, X. Yuan, S. Li, L. Zeng, J. Gong, *Nanoscale* **2015**, 7, 7593.
- [30] H. Wang, W. Fan, Y. He, J. Wang, J.N. Kondo, T. Tatsumi, *J. Catal.* **2013**, 299, 10.
- [31] G. Zhao, M. Deng, Y. Jiang, H. Hu, J. Huang, Y. Lu, *J. Catal.* **2013**, 301, 46.
- [32] G. Zhao, H. Hu, M. Deng, Y. Lu, *Chem. Commun (Camb)* **2011**, 47, 9642.
- [33] S.A. Nikolaev, A.V. Chistyakov, M.V. Chudakova, E.P. Yakimchuk, V.V. Kriventsov, M.V. Tsodikov, *J. Catal.* **2013**, 297, 296.
- [34] H. Tang, F. Liu, J. Wei, B. Qiao, K. Zhao, Y. Su, C. Jin, L. Li, J.J. Liu, J. Wang, T. Zhang, *Angew. Chem. Int. Ed.* **2016**, 55, 10606.
- [35] N. Salam, B. Banerjee, A. S. Roy, P. Mondal, S. Roy, A. Bhaumik, S. Manirul Islam, *Appl. Catal. A: General*, **2014**, 477, 184.
- [36] H. Wei, J. Li, J. Yu, J. Zheng, H. Su, X. Wang, *Inorg. Chim. Acta*, **2015**, 427, 33.
- [37] T. Ghosh, P. Chandra, A. Mohammad, S. M. Mobin, *Appl. Catal. B: Environmental*, **2018**, 226, 278.
- [38] C. H. Tsai, M. Xu, P. Kunal, B. G. Trewyn, *Catal. Today*, **2018**, 306, 81.
- [39] R. Radhakrishnan, S. Thiripuranthagan, A. Devarajan, S. Kumaravel, E. Erusappan, K. Kannan, *Appl. Catal. A, General*, **2017**, 545, 33.
- [40] N. Huo, H. Ma, X. Wang, T. Wang, G. Wang, T. Wang, L. Hou, J. Gao, J. Xu, *Chin. J. Catal.*, **2017**, 38, 1148.

Fig. 1 The yield of methyl benzoate vs the chlorine concentration of the aqueous solution from which the catalyst samples were prepared.

Fig. 2 N₂ adsorption-desorption isotherms of Au/NiOx-22, Au/NiOx-9, and Au/NiOx-3.

Fig. 3 XPS spectra of Au_{4f} (a) and Ni_{2p} (b) of three typical catalysts

Fig. 4 HR-TEM (left) images and size distributions (right) of Au/NiOx-22 (a), Au/NiOx-9 (c), and Au/NiOx-3 (e).

Fig. 5 Fourier transformed (FT) spectra of Au L_{III}-edge (a) and Ni k-edge (b) EXAFS of Au/NiOx-22, Au/NiOx-9, and Au/NiOx-3.

Fig. 6 The simple scheme of Au/NiOx catalysts

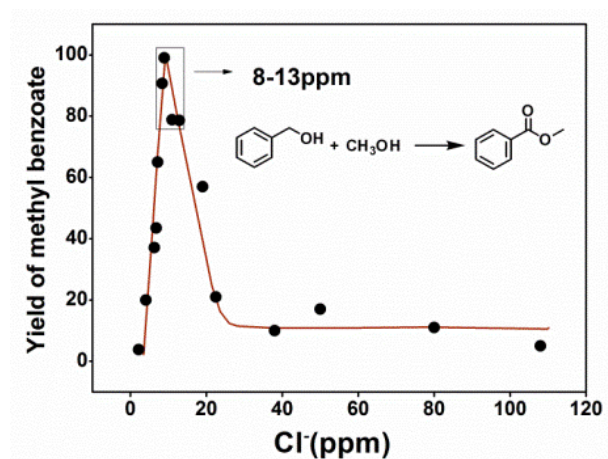


Fig. 1

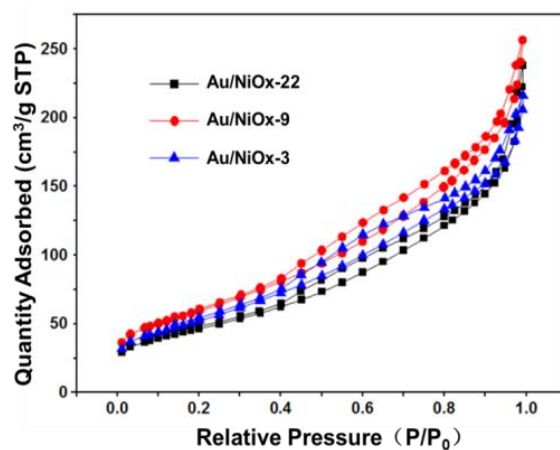


Fig. 2

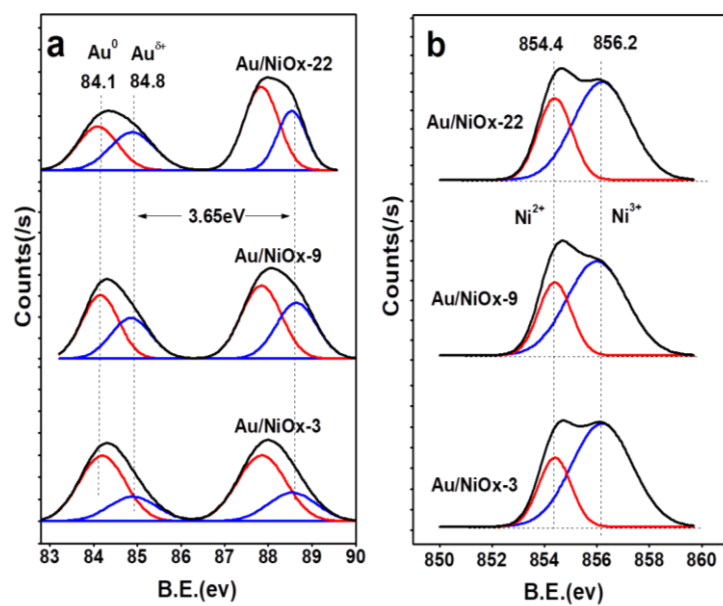


Fig. 3

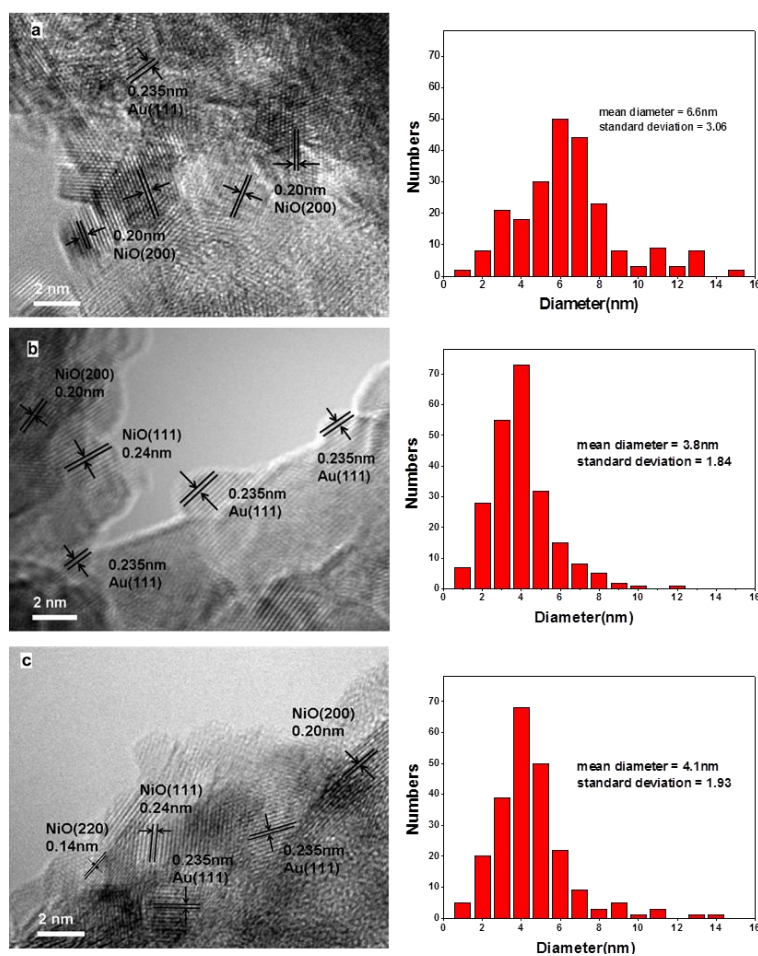


Fig. 4

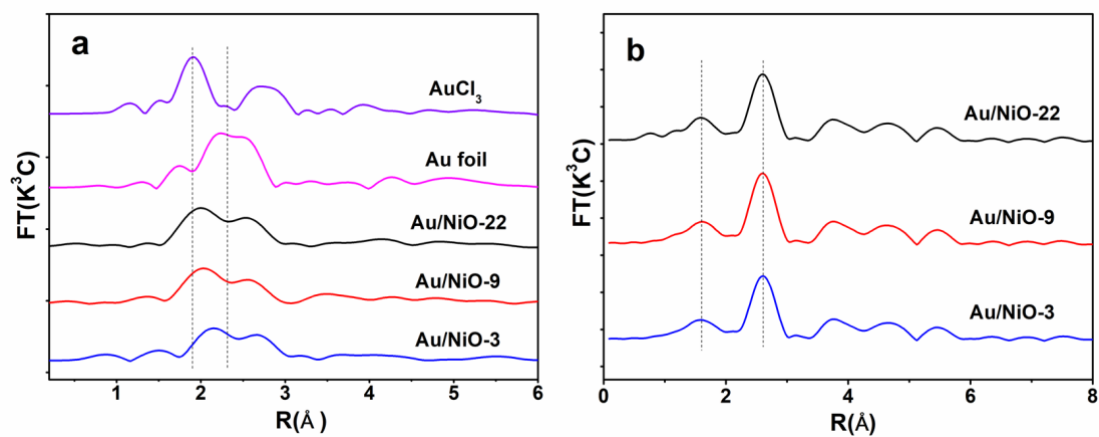


Fig. 5

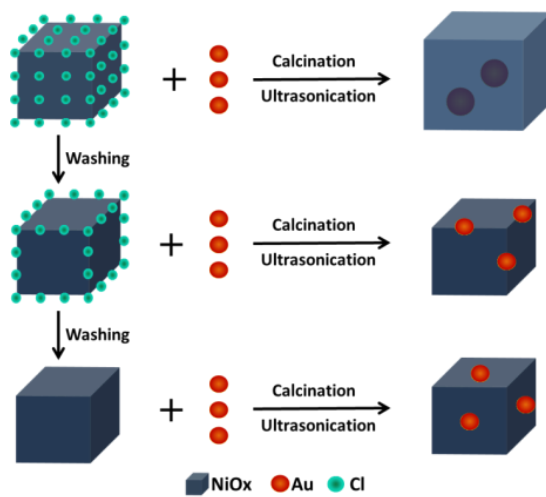


Fig. 6